Secreted Frizzled-related Protein 2 (sFRP2) Redirects Non-canonical Wnt Signaling from Fz7 to Ror2 during Vertebrate Gastrulation[*]

Eva-Maria Brinkmann[‡], Benjamin Mattes[§], Rahul Kumar[‡], Anja I. H. Hagemann[§], Dietmar Gradl[¶], Steffen Scholpp[§], Herbert Steinbeisser[‡], Lilian T. Kaufmann[‡1], and Suat Özbek[‖2]

From the [‡]Institute of Human Genetics, Department of Developmental Genetics, University Hospital Heidelberg, 69120 Heidelberg, Germany, the [§]Karlsruhe Institute of Technology, Institute of Toxicology and Genetics, 76344 Karlsruhe, Germany, the [¶]Zoological Institute, Department of Cell and Developmental Biology, Karlsruhe Institute of Technology, 76131 Karlsruhe, Germany, and the [‖]Centre of Organismal Studies, Department of Molecular Evolution and Genomics, University of Heidelberg, 69120 Heidelberg, Germany

Convergent extension movements during vertebrate gastrulation require a balanced activity of non-canonical Wnt signaling pathways, but the factors regulating this interplay on the molecular level are poorly characterized. Here we show that sFRP2, a member of the secreted frizzled-related protein (sFRP) family, is required for morphogenesis and *papc* expression during *Xenopus* gastrulation. We further provide evidence that sFRP2 redirects non-canonical Wnt signaling from Frizzled 7 (Fz7) to the receptor tyrosine kinase-like orphan receptor 2 (Ror2). During this process, sFRP2 promotes Ror2 signal transduction by stabilizing Wnt5a-Ror2 complexes at the membrane, whereas it inhibits Fz7 signaling, probably by blocking Fz7 receptor endocytosis. The cysteine-rich domain of sFRP2 is sufficient for Ror2 activation, and related sFRPs can substitute for this function. Notably, direct interaction of the two receptors via their cysteine-rich domains also promotes Ror2-mediated *papc* expression but inhibits Fz7 signaling. We propose that sFRPs can act as a molecular switch, channeling the signal input for different non-canonical Wnt pathways during vertebrate gastrulation.

Wnt signaling plays a crucial role in embryogenesis as well as in adult stem cell regulation and cancer. The Wnt signaling cascade is initiated by binding of secreted Wnt proteins to seven-pass transmembrane Fz[3] receptors and diverse co-recep-tors. The extracellular CRD of Fz family members thereby serves as a highly conserved binding site for Wnt ligands (1–3). Wnt proteins can activate different branches of Wnt signaling depending on the particular Wnt ligand and/or receptor involved and the cellular context. The canonical Wnt/β-catenin pathway requires a ternary complex of Wnt-Fz and a co-receptor of the LDL receptor-related protein family (LRP5 or LRP6). The β-catenin-independent, non-canonical Wnt calcium (Wnt/Ca^{2+}) or planar cell polarity (PCP) pathways rely on different co-receptors, such as Ror2, Ryk, and Vangl, and down-stream signaling factors (4).

sFRPs can modulate Wnt signaling by binding to Wnt ligands and Fz receptors (5). They are soluble glycoproteins of ~300 amino acids in length and contain an N-terminal CRD homologous to Fz receptor CRDs and a C-terminal netrin-like (NTR) domain. sFRPs are described as inhibitors of the canonical Wnt/β-catenin pathway by competing with Fz receptors for Wnt binding (6–9).

In vertebrates, the Wnt/PCP pathway is a key regulator of cell movements, such as CE movements, which are required during vertebrate gastrulation to establish the embryonic body plan (10). Fz7 acts as main β-catenin-independent receptor and triggers Wnt/PCP signaling by activating the small GTPases RhoA, Rac1, and JNK upon Wnt ligand binding (11). Recent studies have shown that Wnt/PCP signal transduction requires the internalization of Fz receptors (12, 13). However, the molecular mechanism regulating the process of Wnt/Fz endocytosis and downstream signaling is not fully understood.

In addition to classical Fz7-mediated, β-catenin-independent signaling, a further branch mediated by Ror2 is required for CE movements (14–16). Ror2 is a single-pass transmembrane receptor tyrosine kinase and contains an N-terminal CRD that interacts with Wnt5a. Previous data show that Ror2 induces the expression of paraxial protocadherin (*papc*) and requires Ror2 tyrosine kinase activity (17, 18). *papc* encodes a transmembrane protocadherin and plays a crucial role in CE movements that drive *Xenopus* gastrulation. It has homotypic cell adhesion activity and is required to establish segmental boundaries (19, 20). Thus, in addition to Fz7-mediated activation of RhoA and Rac1 (16), the Wnt5a/Ror2 pathway has been suggested to form an additional branch of the β-catenin-inde-

[3] The abbreviations used are: Fz, Frizzled; CRD, cysteine-rich domain; PCP, planar cell polarity; sFRP, secreted frizzled-related protein; NTR, netrin-like domain; ECD, extracellular domain; CE, convergent extension; Mo, morpholino(s); AC, animal cap; DMZ, dorsal marginal zone; qPCR, quantitative PCR; IP, immunoprecipitation; KD, kinase-dead; WB, Western blotting; ATF, activating transcription factor; TK, thymidine kinase.

pendent signaling network, likely requiring PI3K, CDC42, and MKK7 to activate JNK signaling (16). There is accumulating evidence for a role of sFRPs in non-canonical Wnt signaling. It was demonstrated that, in mice, sFRP1 and sFRP2 regulate anterior-posterior axis elongation and PCP processes during early trunk formation (21, 22). Moreover, sFRP5 as well as sFRP2 can directly disrupt Wnt/PCP signaling (23, 24). Whether this inhibition is a general role of sFRPs or whether they have distinct functions in the different β-catenin-independent Wnt signaling branches remains unknown.

In this study, we investigate the role of sFRP2 during early *Xenopus* and zebrafish development and provide insights into the function of sFRPs in two distinct branches of β-catenin-independent Wnt signaling. We found that sFRP2 regulates CE movements and additional β-catenin-independent Wnt signaling events during *Xenopus* gastrulation. Notably, sFRP2 inhibits Fz7-mediated signaling while potentiating Ror2-mediated expression of *papc*. We also provide evidence that Fz7 and/or an sFRP are required for *papc* expression. Consistently, we show that, in the presence of Fz7, Ror2 signaling activity is enhanced. Furthermore, we demonstrate that, in zebrafish embryos, sFRP2 and Ror2 prevent the internalization of Fz7 upon Wnt5a stimulation, suggesting repression of Fz7-mediated non-canonical signaling by blocking its endocytosis. Our findings suggest that sFRP2 functions as a molecular switch between Ror2 and Fz7 signaling during vertebrate development.

Experimental Procedures

Plasmids, Constructs, and mRNA Synthesis—Capped mRNAs for microinjections were transcribed from linearized plasmids using the SP6 or T7 mMessagemMachine kit from Ambion. The plasmids used in this study were as follows: pCS2+NT7C5 (25), pCS2+Fz7 and pCS2+Fz7-myc (26); pCS2+Ror2, pCS2+Ror2 KD (18), pCS2+Wnt5a (27), and pCS2+Wnt11 (28). Furthermore, the following clones were provided by Andrey Glinka: pCS2+Dkk3-HA, pCS2+mouse Ror2-myc, and pCS2+mouse Ror2 ECD-FLAG. pCS2+sFRP2-HA was provided by Anne Gorny and pCS2+Ror2-HA by Doris Wedlich. pCMV-SPORT6+human sFRP2 was obtained from Invitrogen (accession no. NM_003013). The pCS2+sFRP2 CRD-HA deletion construct was generated from full-length pCS2+sFRP2-HA by PCR amplification using the following primers: 5′-GCTCCTCTTCTAAGAAAACTCG-3′ and 5′-CGATCT-CCTTCACTTTTATCTTC-3′. The amounts of synthetic mRNAs injected in the different experiments are indicated in the figure legends.

Antisense Morpholino Oligonucleotides—All antisense morpholino oligonucleotides (Mo) used in this study were ordered from Gene Tool LLC. sFRP2 Mo (5′-AGCGCGACCCGCT-GTGCCACATGAT-3′) covers the ATG region of x*sfrp2* (BJ071409). All other Mo were described previously: Fz7 Mo (29), Ror2 Mo, standard Mo (16), sFRP1 Mo (30), and frzb2 (crescent) Mo (31). All antisense Mo were injected with a concentration of 15 ng/embryo.

Xenopus Embryo Manipulation—*Xenopus laevis* frogs were obtained from Nasco. All experiments complied with local (Regierungspräsidium Karlsruhe, Az.35-9185.82) and interna-

tional guidelines for the use of experimental animals. Embryos were essentially obtained by *in vitro* fertilization, microinjected, and cultured as described previously (32). The injection sites, construct compositions, and stages used in the individual experiments are indicated in the figure legends and in the following sections.

Animal Cap Elongation Assay—For animal cap (AC) explants, embryos were injected at the two-cell stage into both blastomeres, close to the animal pole. ACs were dissected at stage 8.5 and cultivated overnight in 0.5× modified Barth solution high salt (MBSH) together with 10 ng/μl gentamycin and 50 ng/μl Activin on plates coated with BSA. For the analysis of *xbra* expression, AC explants were cultivated only for 2 h in Activin before total RNA was extracted for qPCR. When control embryos reached stage 26, the ACs were fixed in Eagle's minimal essential medium with 3.7% formaldehyde (MEMFA) and scored for elongation. Elongated explants were classified into three subgroups: full elongation, partial elongation, and no elongation.

RT-PCR and Quantitative Real-time PCR—Total RNA from five whole embryos at stage 11 or 10 caps, dissected at stage 8.5 and cultivated until control embryos reached stage 12, was extracted using the MasterPure RNA purification kit (Epicenter Biotechnologies). cDNA was then synthesized using random hexamer primers and reverse transcriptase RT Maxima (Fermentas). Real-time PCR was carried out using SYBR Green mix (Thermo Scientific). Expression levels were normalized to *ornithin-decarboxylase* (*odc*). The primers were as follows: *odc*, 5′-TGCACATGTCAAGCCAGTTC-3′ and 5′-GCCCATCA-CACGTTGGTC-3′; *xnr3*, 5′-CCAAAGCTTCATCGCTAA-AAG-3′ and 5′-AAAAGAAGGGAGGCAAATACG-3′; *papc*, 5′-CCCAGTCGGTCTCTTCTTCTTTG-3′ and 5′-TTGCT-GATGCTGCTCTTGGTTAG-3′; *xbra*, 5′-TTCAGCCTGTC-TGTCAATGC-3′ and 5′-TGAGACACTGGTGTGATGGC-3′; and *ror2*, 5′-GGAGCAACTCCTAGAGG-3′ and 5′-GAG-TGGATTCCCGGACACT-3′.

Luciferase Reporter Assay—For the ATF luciferase reporter assay, four-cell stage embryos were injected into both animal ventral blastomeres with 100 pg of ATF2-firefly luciferase reporter plasmid (44) in combination with 10 pg of pRL-TK (thymidine kinase promoter) *Renilla* luciferase reporter plasmid (Promega). The reporter plasmids were injected alone or together with the indicated synthetic mRNAs. Luciferase reporter assays were carried out from whole embryos lysed at gastrula stage (stage 12). Triplicates of five embryos each were lysed in 125 μl of passive lysis buffer (Promega), and 20 μl of this embryo lysate was used to quantify luciferase activity using the Dual-Luciferase system (Promega) according to the instructions of the manufacturer.

Whole Mount in Situ Hybridization—The antisense probe against *papc* was synthesized from the pBS+PAPC full-length clone (19) and linearized with XbaI, and T7 RNA polymerase was used for *in vitro* transcription. For whole-mount *in situ* hybridizations, four-cell stage embryos were injected into the DMZ with morpholinos and/or synthetic mRNAs. After gastrula embryos were fixed in MEMFA, they were hybridized with antisense probes against *papc*. Digoxigenin/alkaline phospha-

tase (Roche) was used as a detection system, and *in situ* hybridization was performed as described previously (33).

Immunoprecipitation, SDS-PAGE, and Western Blotting—For immunoprecipitation (IP) experiments in HEK293T cells, 1 μg of the corresponding plasmids was transfected using Turbofect transfection reagent (Thermo Scientific). pCS2+mRor2-myc or pCS2+Fz7-myc was transfected alone or in combination with pCS2+sFRP2-HA. The pCS2+GFP plasmid was used as a transfection control and to adapt transfected plasmid amounts. After cells were lysed, the protein lysate was divided into three separate aliquots either incubated with a mouse anti-IgG antibody (Dianova), anti-myc antibody (1:100, Calbiochem), or a mouse anti-HA antibody (1:100, Sigma) to precipitate the corresponding tagged proteins.

For the Ror2/Wnt5a-V5 binding assay in HEK293T cells, 1 μg of pCS2+mouse Ror2 ECD-FLAG was transfected alone or in combination with either pCS2+sFRP2-HA, pCS2+sFRP2 CRD-HA, pCS2+Fz7-myc, pCS2+Dkk3-HA, or pCS2+GFP. For the Fz7-myc/Wnt5a-V5 binding assay in HEK293T cells, 1 μg of Fz7-myc was transfected alone or in combination with either pCS2+sFRP2-HA, pCS2+Ror2-HA, or pCS2+GFP. After 48 h of incubation, cells were washed with serum-free medium and then further incubated with Wnt5a-V5 conditioned medium stably secreted by L-cells (34) for 15 min. Cells were lysed in NOP buffer (150 M NaCl, 10 mM Tris/HCl (pH 7.8), 1 mM $MgCl_2$, 0.75 mM $CaCl_2$, 1% Nonidet P-40, and 0.3 mM OGP), followed by incubation with rabbit anti-FLAG (OctA probe, Santa Cruz Biotechnology) or rabbit anti-myc (Millipore). After rotation for 2 h at 4 °C, 50 μl of magnetic bead suspension (Adamtech) was added to the cell lysate, and it was further incubated overnight at 4 °C. After washing the precipitated proteins several times with ice-cold lysis buffer, lysates were resuspended in PAG elution buffer (Adamtech). For co-IP with secreted proteins, conditioned media were generated from HEK293T cells transfected with either sFRP2-HA or Ror2-ECD-FLAG. Proteins were then purified separately using magnetic beads coupled to a mouse anti-HA (MBL) or mouse anti-FLAG (MBL) antibody, respectively, and incubated overnight at 4 °C. The samples were then washed several times with lysis buffer, and bound proteins were eluted with 0.2 M glycine in PBS (pH 3.0). Purified proteins were then mixed, diluted with DMEM, and incubated for 1 h at 4 °C to allow binding. This complex was further incubated with a mouse anti-HA antibody (Sigma) and 40 μl of magnetic bead suspension (Adamtech) for 3 h at 4 °C. After washing the precipitated proteins several times with ice-cold lysis buffer, lysates were resuspended in PAG elution buffer (Adamtech).

Proteins were separated by 15% SDS-PAGE. For Western blotting analysis, a mouse anti-myc (1:1000, Calbiochem), mouse anti-V5 (1:1000, Invitrogen), mouse anti-FLAG (1:1000, Sigma), rabbit anti-FLAG (Octaprobe), or mouse anti-HA antibody (1:1500, Sigma) was used.

Microinjection and Fluorescence Analysis in Zebrafish and Xenopus—All zebrafish husbandry and experimental procedures were performed in accordance with the German law on animal protection and approved by the local animal protection committee (Regierungspräsidium Karlsruhe, Az.35-9185.64) and the Karlsruhe Institute of Technology. Breeding zebrafish (*Danio rerio*) were maintained at 28 °C on a 14-h light/10-h dark cycle (35). The data we present in this study were acquired from analysis of Karlsruhe Institute of Technology wild-type zebrafish AB_2O_3.

Embryos were harvested and enzymatically dechorionated with Pronase (Sigma-Aldrich) at the one-cell stage before injection. All indicated constructs were injected at the one-cell stage as capped mRNA *in vitro* transcribed with the mMessage Machine kit (Ambion).

For fluorescence analysis in zebrafish, the following plasmids were used: xWnt5a (16), zf Fz7-CFP (36), xRor2-mCherry, xWnt5a-GFP (37), mem-mCherry, and GFP-GPI (38). For immunohistochemistry of DMZ explants, *Xenopus* embryos were injected into the dorsal equatorial zone at the four-cell stage, and DMZ explants were dissected from gastrula embryos at stage 10. After explants were fixed with 4% formaldehyde, they were stained with the following primary antibodies: rabbit anti-Fz7, mouse anti-HA, mouse anti-myc, or rabbit anti-myc. Anti-rabbit Alexa Fluor 488, anti-mouse Alexa Fluor 488, anti-mouse Alexa Fluor 555, or anti-rabbit Alexa Fluor 555 were used as secondary antibodies.

Microscopy—The embryos and ACs were photographed using a Zeiss Axiophot stereomicroscope and a Leica DC350FX camera. Confocal laser scanning of DMZ explants was done using a Nikon C1 plus laser-scanning microscope. Photoshop was used for further image processing. For confocal analysis, live zebrafish embryos were embedded in 0.7% low-melting agarose (Sigma-Aldrich) dissolved in 1× Ringer's solution. Images were obtained with a Leica TCS SP5 X confocal laser-scanning microscope using ×63 dip-in objectives. Image processing was performed with Imaris v7.5.2 software (Bitplane AG).

Results

Gain and Loss of sFRP2 Impairs CE Movements in Xenopus—sFRP2 is expressed in the dorsal mesoderm of a gastrulating embryo (39), and its expression pattern overlaps with several non-canonical Wnt pathway components, including Wnt11, Wnt5a (31), Fz7, Fz8 (40, 41), and Ror2 (18). Inactivation as well as stimulation of the β-catenin-independent Wnt signaling pathway leads to gastrulation defects such as a shorter anterior-posterior axis or spina bifida (17, 42). To investigate the role of sFRP2 in CE movements, we injected *X. laevis* sfrp2 mRNA and a translation-blocking *sfrp2* antisense Mo (sFRP2 Mo) into *Xenopus* embryos. Both overexpression as well as reduction of sFRP2 caused gastrulation defects (Fig. 1A). Almost all sFRP2 overexpressing embryos showed either a shorter body axis (51%) or spina bifida (45%). Similar to *sfrp2* from *Xenopus*, the human homolog (*hsfrp2*) also induced gastrulation defects, suggesting an evolutionarily conserved function. Furthermore, similar phenotypes were also observed in sFRP2 morphants (Fig. 1, *A* and *B*). Co-injection of human *sfrp2* (*hsfrp2*) mRNA partially rescued the sFRP2 Mo loss-of-function phenotype, indicating that well balanced levels of sFRP2 are required for proper gastrulation.

To support the finding that sFRP2 affects CE movements during *Xenopus* gastrulation, we performed an elongation assay using Activin-treated AC explants. Consistent with published
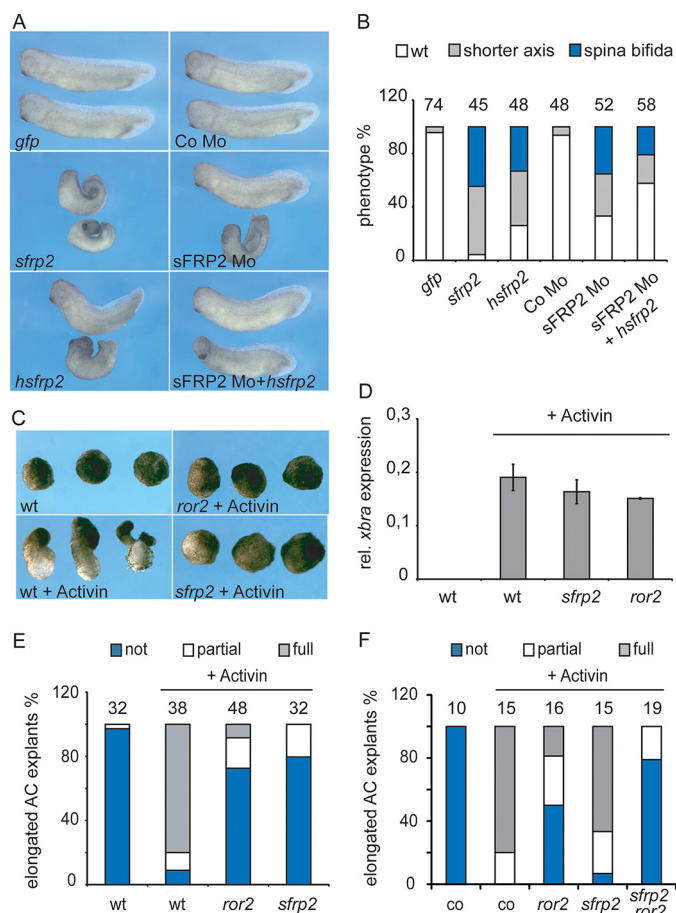
FIGURE 1. **Gain and loss of sFRP2 impairs CE movements in *Xenopus*.** *A*, representative phenotypes of embryos injected into the dorsal equatorial zone at the four-cell stage with the indicated Mo (15 ng) and synthetic mRNA (500 pg of *sfrp2/hsfrp2* or 200 pg for the Mo rescue). *B*, quantification of the phenotypic analysis shown in *A*. The numbers of analyzed embryos are indicated on top of the *columns*. *C*, for the AC elongation assay, embryos were injected at the two-cell stage with the indicated synthetic mRNAs (300 pg) and excised at stage 9. ACs were cultured with or without Activin overnight to analyze elongation. *D*, analysis of *xbra* expression of 10 ACs as shown in *C*, harvested after 2-h incubation in Activin. Shown is a representative with technical triplicates. This was confirmed by at least two independent experiments with similar results using sibling animal caps of those shown in *C* and *E*. *E*, quantification of the AC elongation shown in *C* and categorized as not elongated (*blue*), partially elongated (*white*), and fully elongated (*gray*) ACs. The numbers of analyzed ACs are indicated on top of the *columns*. *F*, AC elongation assay of embryos injected with 100 pg of each indicated synthetic mRNA. To balance injected mRNA quantities, the respective amount of *gfp* mRNA was co-injected. Scoring and quantification was as in *C* and *E*. *Co*, control.

FIGURE 2. **sFRP2 is required for *papc* expression and enhances Ror2-mediated signaling.** *A*, representative *papc* expression pattern analyzed by whole mount *in situ* hybridization of gastrula (stage 10.5) embryos injected at the four-cell stage in the dorsal equatorial region with the indicated Mo (15 ng). *Arrowheads* indicate the site of injection. *Co*, control. *B*, quantification of *in situ* hybridization shown in *A*. The numbers of analyzed embryos are indicated on top of the *columns*. *C* and *D*, relative (*rel*) expression of *papc* analyzed by qPCR in whole embryos injected with the indicated Mos (15 ng) and synthetic mRNA (200 pg). *E* and *F*, relative expression of *papc* analyzed by qPCR in AC explants injected with the indicated synthetic mRNAs (500 pg of *ror2/sfrp2* and 150 pg of *wnt5a*). *G*, relative expression of *ror2* in ACs from uninjected embryos cut at stage 9 and harvested after 14 h with or without Activin (50 ng/ml). *H*, ATF luciferase reporter assay of stage 12 gastrula embryos injected with the indicated synthetic mRNAs (500 pg of *ror2/sfrp2* and 100 pg of *wnt5a*) and the ATF2 firefly and pRL-TK *Renilla* luciferase reporter constructs. *C* and *G* show the mean ± S.D. of three independent experiments. *, *p* < 0.05 compared with controls. *D–F* show a representative with technical triplicates. This was confirmed by at least two (*D* and *F*) or three (*E*) independent experiments in different batches of *X. laevis* with similar results. *H* shows the mean ± S.D. of biological triplicates of pools of seven embryos each (*, *p* < 0.05 compared with controls). This was confirmed in at least three independent experiments in different batches of *X. laevis*.

data, Ror2 overexpression inhibited AC elongation and served as a positive control in this assay (18). Like Ror2, sFRP2 efficiently blocked the elongation of Activin-treated ACs (Fig. 1, *C–E*). This inhibition of elongation was caused by disruption of cell movements and not by interference with mesoderm induction because neither Ror2 nor sFRP2 overexpression affected the induction of the mesodermal marker gene *Xbra* (Fig. 1*D*) (43). Interestingly, injection of low amounts of *sfrp2* mRNA repressed elongation only slightly (Fig. 1*F*). In combination with equally low amounts of *ror2* mRNA, however, nearly full inhibition was reached, indicating that sFRP2 and Ror2 cooperate during CE movement (Fig. 1*F*).

sFRP2 Is Required for papc Expression and Enhances Ror2-mediated Signaling—Because our results show that sFRP2 influences cell movements during *Xenopus* gastrulation, we
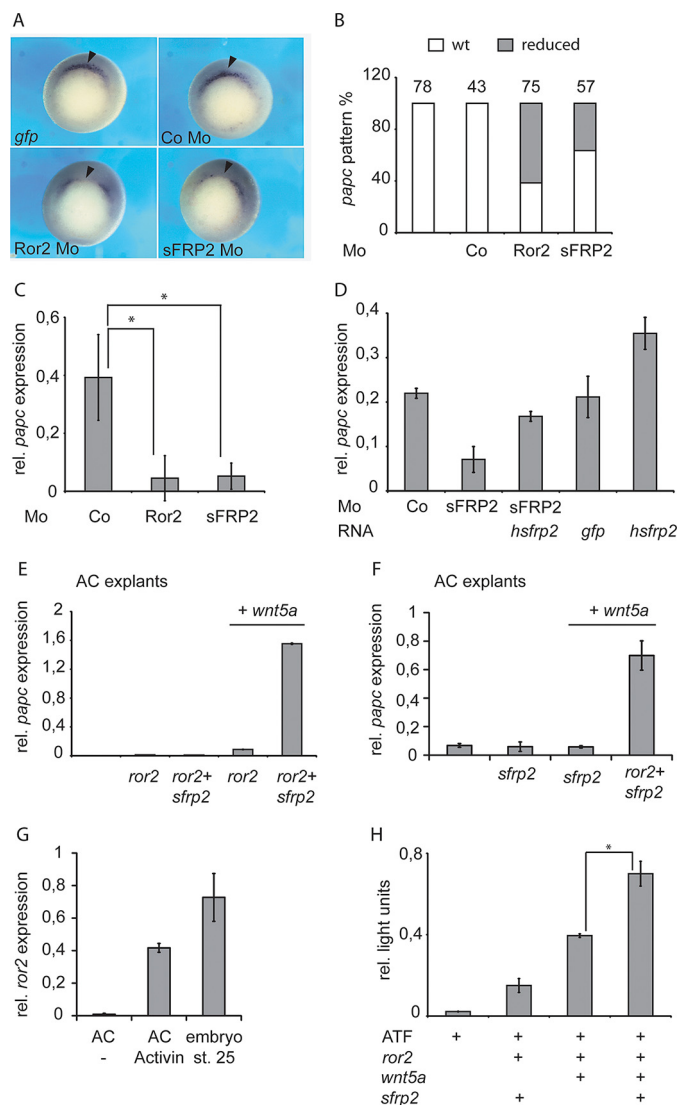
next investigated its effect on the relevant pathways. We decided to focus first on Wnt5a/Ror2 signaling and analyzed the effect of sFRP2 on the activation of Wnt5a/Ror2-mediated *papc* induction (16).

For this purpose, sFRP2 Mo was injected into the dorsal equatorial region of four-cell stage embryos, and the expression pattern of *papc* was evaluated at the gastrula stage (Fig. 2, *A* and *B*). We found that sFRP2-deficient embryos had reduced *papc* expression at the dorsal lip, similar to Ror2-deficient embryos (Fig. 2*A*). Loss of Ror2 reduced *papc* levels in 61% ± 8% of the embryos and loss of sFRP2 in 39% ± 2% of the embryos (Fig. 2*B*). Consistently, sFRP2 overexpression led to increased *papc* expression (data not shown). To verify this observation, *papc* expression was further analyzed using qPCR. Concurrently, loss of sFRP2 mimicked the loss of Ror2 and resulted in a significant decrease of *papc* transcription (Fig. 2*C*), whereas *hsfrp2* up-regulated *papc* (Fig. 2*D*). Co-injection of the morpholino and *hsfrp2* restored *papc* expression to almost WT levels (Fig. 2*D*). These findings show that sFRP2 regulates *papc* expression during *Xenopus* gastrulation.

To examine whether sFRP2 is able to enhance Wnt5a/Ror2 signaling directly, we used *Xenopus* AC explants. In WT ACs excised at blastula stage, only very few transcripts of *papc* are expressed, and ectopic expression of Ror2 and Wnt5a induce the transcription of *papc* (16). Indeed, we could show that sFRP2 strongly enhanced Wnt5a/Ror2-mediated *papc* expression compared with the level induced by Wnt5a/Ror2 alone (Fig. 2*E*). This up-regulation of *papc* strictly depends on the presence of Wnt5a because co-expression of sFRP2 and Ror2 alone could not induce *papc* (Fig. 2*E*). sFRP2 overexpression alone was not able to induce *papc* expression in AC explants both in the presence and absence of Wnt5a (Fig. 2*F*). Because, in Activin-treated AC explants, sFRP2 overexpression alone interfered with CE movement (Fig. 1, *C–E*), we analyzed the expression of *ror2* in AC explants after mesoderm induction. As expected, *ror2* was induced in AC explants treated with Activin but was not expressed in unstimulated explants (Fig. 2*G*).

To confirm the potentiating effect of sFRP2 on Ror2 signaling, we used the ATF luciferase reporter assay, which is based on JNK-dependent phosphorylation and therefore serves a readout system for β-catenin-independent Wnt signaling (44). In line with our previous observation, sFRP2 augmented Wnt5a/Ror2-mediated ATF activity (Fig. 2*H*). Taken together, these findings demonstrate that sFRP2 is a positive modulator of Wnt5a/Ror2 signaling.

sFRP2 Interacts with Ror2 and Stabilizes Wnt5a-Ror2 Complexes—To investigate whether the molecular mechanism underlying the observed positive modulation of Wnt5a/Ror2 signaling by sFRP2 occurs via interaction of sFRP2 with the ligand-receptor complex, we performed binding studies in HEK293T cells. In co-IP assays using myc-tagged Ror2 and HA-tagged sFRP2, we demonstrate that sFRP2 forms a complex with Ror2 (Fig. 3*A*). We confirmed the observed interaction between Ror2 and sFRP2 additionally by using purified proteins from conditioned media generated in HEK293T cells (Fig. 3*B*).

We propose that interaction of sFRP2 with Ror2 increases Ror2-mediated signaling. It was demonstrated previously that association of Fz7 with Ror2 enhances the affinity of Wnt5a to Ror2 and is required for Wnt5a/Ror2 signaling to induce the activation of AP-1 (JNK/c-jun) (45).

Because the CRDs of Fz receptors and sFRPs are homologous, we tested whether sFRP2, similar to Fz7, can enhance Wnt5a binding to Ror2. HEK293T cells were either transfected with Ror2 alone or co-transfected with sFRP2, sFRP2-CRD, or Fz7 as a positive control. After stimulating the cells with equal amounts of Wnt5a-conditioned medium, we compared the levels of Wnt5a co-precipitated with Ror2. In the absence of Fz-CRD-containing proteins, only traces of Wnt5a were associated with Ror2 (Fig. 3*C*). However, when sFRP2 or its CRD were co-expressed, significantly more Wnt5a co-precipitated with Ror2. This increase was even stronger than the increase observed in the presence of Fz7 (Fig. 3*C*). However, this is not surprising because also more sFRP2 and sFRP2-CRD precipitated with Ror2 compared with Fz7 (Fig. 3*D*). As a control protein containing an unrelated cysteine-rich domain we used Dkk3, which does not bind to Ror2 (Fig. 3*D*) and hence did not increase Wnt5a binding to Ror2 (Fig. 3*C*).

The stabilizing effect of sFRP2 on Wnt5a was further confirmed *in vivo* using fluorescently tagged proteins in zebrafish embryos. In the absence of sFRP2, only a low level of Wnt5a-GFP co-localized with Ror2-mCherry at the membrane (Fig. 3*E*). However, co-expression of sFRP2 resulted in a stronger formation of Ror2-mCherry-Wnt5a-GFP-positive puncta at the plasma membrane, seen by an increase of 65.8% ± 19.2% (S.E.) of the fluorescent signal of Wnt5a-GFP (Fig. 3*E*). Taken together, our data suggest that sFRP2 specifically binds to Ror2 via its CRD and thereby increases the recruitment of Wnt5a to Ror2 receptor complexes at the plasma membrane, as indicated by stabilized Wnt5a-Ror2 complex formation.

sFRPs and Fz7 Act Redundantly in Ror2 Activation—We showed that sFRP2 interacts with Ror2 and is able to enhance Wnt5a-Ror2 complex formation. The CRD of sFRP2 is highly homologous to those of other secreted Wnt modulators of the sFRP family. This prompted us to analyze whether these sFRPs are also involved in *papc* transcription. Indeed, knockdown of sFRP1 and frzb2 reduced the expression of *papc* compared with control embryos, suggesting that sFRP1 and frzb2 positively modulate Ror2 signaling (Fig. 4*A*). In contrast, knockdown of Dkk1, a secreted modulator of Wnt/β-catenin signaling, had no influence on the expression of *papc* (data not shown). Moreover, we observed that frzb2 could rescue the sFRP2 Mo phenotype (Fig. 4*B*), indicating that they function redundantly.

Consistent with our hypothesis that Fz-CRDs enhance Wnt5a-Ror2 signaling, knockdown of Fz7 reduced the level of *papc* in qPCR (Fig. 4*A*) and in whole mount *in situ* hybridization experiments (Fig. 4*C*). Loss of Fz7 therefore mimics loss of sFRP2. This suggests that both receptors also co-operate *in vivo*, in line with the known role of Fz7 in Wnt5a-Ror2-induced AP-1 activation *in vitro* (45). Next, we investigated whether Fz7 has an effect on Ror2-induced signaling in AC explants and found that Wnt5a/Ror2-mediated induction of *papc* is further enhanced by co-injection of *fz7* mRNA (Fig. 4*D*). Notably, in the absence of Ror2, Fz7 was unable to induce *papc* expression in ACs, confirming that *papc* is a Ror2-specific target gene, as published earlier (16). We further show that endogenous Fz7 co-localizes with Ror2-myc and sFRP2-HA at the membrane in DMZ explants during *Xenopus* gastrulation (Fig. 4*E*). We hypothesize that the presence of a CRD motif is required to stabilize the Wnt5a-Ror2 signaling complex whether it is provided by the Fz7 receptor or secreted Fz-related modulators.

FIGURE 3. **sFRP2 interacts with Ror2 in HEK293T cells and stabilizes Wnt5a-Ror2 complexes.** *A*, co-IP in HEK293T cells transfected with Ror2-myc- and HA-tagged sFRP2 (1 μg of each). Protein lysates were precipitated with a mouse antibody against myc or HA, respectively, and IgG as a negative control. Western blotting (WB) analysis with anti-HA antibody shows that sFRP2 is pulled down together with Ror2. *B*, IP from conditioned media generated in HEK293T cells transfected with either Ror2 ECD-FLAG or sFRP2-HA. Purified proteins were mixed and further precipitated with a mouse anti-HA antibody. WB analysis with rabbit anti-FLAG shows that purified sFRP2 binds to purified Ror2-ECD. As a negative control (*Ctrl*), Ror2 ECD-FLAG conditioned medium was precipitated with anti-HA-coupled magnetic beads and sFRP2-HA conditioned medium with anti-FLAG-coupled magnetic beads. *C*, the Wnt5a-V5 binding assay was performed in HEK293T cells transfected with Ror2 ECD-FLAG alone or co-transfected with sFRP2-HA, CRD-HA, DKK3-HA, or Fz7-myc (1 μg of each). Each cell sample was treated with equal amounts of Wnt5a-V5 conditioned medium for 15 min before cells were lysed for rabbit anti-FLAG pulldown to precipitate Ror2. The samples were then analyzed on two different WBs. The WB on top was analyzed with anti-V5 antibody for the Wnt5a-V5 fraction bound to precipitated Ror2-FLAG. The bottom WB was analyzed with mouse anti-FLAG and shows that equal amounts of Ror2 were precipitated in the different samples. *D*, the WB analyzed with mouse anti-HA/anti-myc antibody shows that all co-transfected proteins were expressed (*input*, *first four lanes*) and were co-precipitated with the Ror2-FLAG pulldown (*IP*, *α-FLAG*, *last four lanes*). Only Dkk3 was not precipitated with Ror2. A schematic of the different proteins used in the experiment is shown below. sFRP family proteins are related to Fz receptors in the CRD. *TM*, transmembrane domain; *CD*, cytoplasmic domain; *Cys*, cysteine-rich domain. *E*, confocal microscopy analysis of live zebrafish embryos expressing 1 ng of mRNA of the indicated constructs at 30–50% epiboly stages shown in the indicated colors. Confocal images represent single z sections. Ror2-mCherry shows membrane localization regardless of the presence of Wnt5a or sFRP2. Wnt5a-GFP shows co-localization with Ror2-mCherry in discrete clusters at the membrane. Co-expression of sFRP2 with Ror2-mCherry/Wnt5a-GFP leads to an enhanced membrane localization of Wnt5a-GFP.

sFRP2 and Ror2 Inhibit Fz7-mediated Signaling—Next we asked how sFRP2 affects Fz7 signaling activity because we observed that sFRP2 co-localized with (Fig. 4*E*) and acts in the same complex with Fz7 (Fig. 5*A*). Because no specific readout or target gene analysis is available for Fz7-mediated signaling, we used a chimeric NT7C5 receptor construct described previ-

ously (25). This chimeric receptor consists of the intracellular domain of human Fz5 and the extracellular and transmembrane domains of Fz7. When stimulated with Wnt5a, this receptor induces the expression of the Wnt/β-catenin target gene Nodal-related (*xnr3*). In contrast, WT *Xenopus* Fz7 cannot activate *xnr3* after Wnt5a stimulation (25). Analysis of the
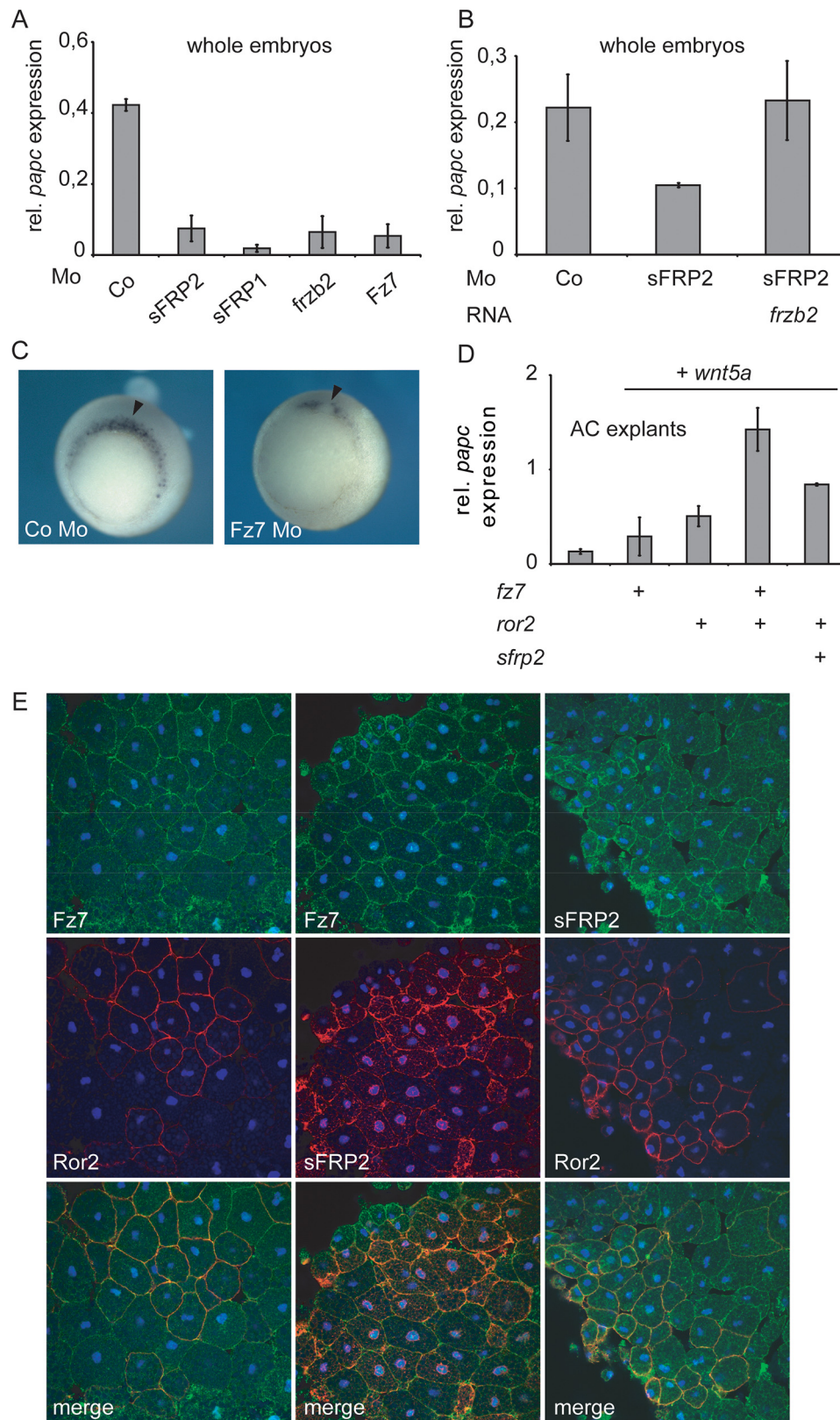
FIGURE 4. **sFRPs and Fz7 act redundantly to activate Ror2.** *A* and *B*, relative (*rel*) expression of *papc* analyzed by qPCR in gastrula stage 10.5 whole embryos injected dorsal-equatorially with the indicated Mo (15 ng) and synthetic mRNA (200 pg). *Co*, control. *C*, *papc* expression of Fz7 morphants analyzed by whole mount *in situ* hybridization of gastrula stage embryos. *Arrowheads* indicate the site of injection. *D*, relative expression of *papc* analyzed by qPCR in AC explants injected with the indicated synthetic mRNAs (500 pg of *ror2/fz7* and 150 pg of *wnt5a*). *A*, *B*, and *D* show a representative with technical triplicates. This was confirmed by at least two independent experiments in different batches of *X. laevis* with similar results. *E*, confocal microscopy analysis of DMZ explants of *Xenopus* embryos injected dorsal-equatorially at the four-cell stage with 500 pg of Ror2-myc or 500 pg of sFRP2-HA. Endogenous Fz7 is shown in *green*, and overexpressed Ror2 and sFRP2 are shown in the indicated colors.
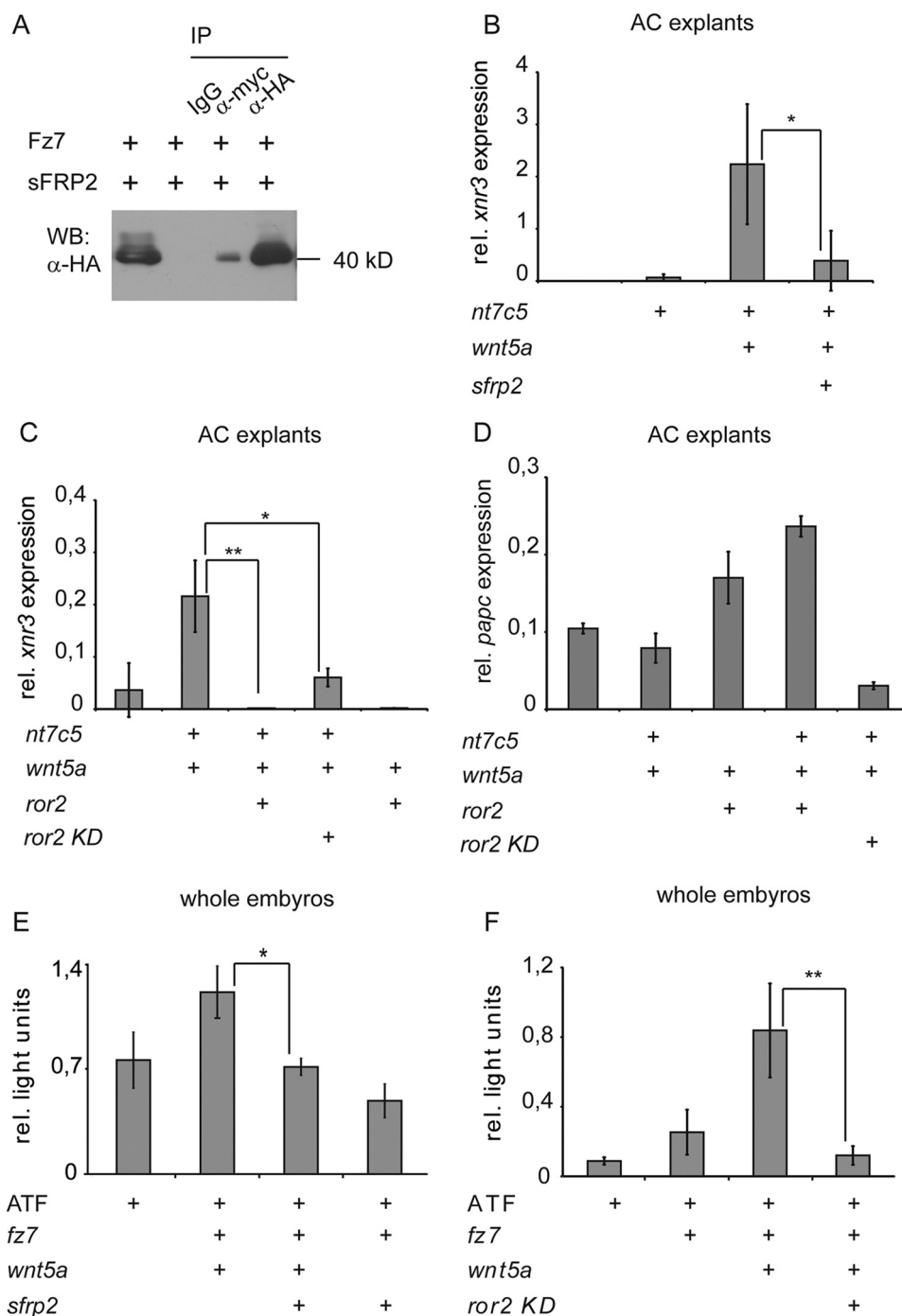
FIGURE 5. **sFRP2 and Ror2 inhibit Fz7 mediated non-canonical Wnt signaling.** *A*, co-IP in HEK293T cells transfected with Fz7-myc and sFRP2-HA (1 μg of each). Protein lysates were precipitated with a mouse antibody against myc or HA, respectively, and IgG as a negative control. WB analyzed with anti-HA antibody shows that sFRP2 is pulled down together with Fz7. *B—D*, qPCR analysis of AC explants of embryos injected with the indicated mRNAs (500 pg of *n7c5/sfrp2/ror2/ror2 kd* and 100 pg of *wnt5a. rel*, relative. *E* and *F*, ATF luciferase reporter assay of stage 12 gastrula embryos injected with the indicated synthetic mRNAs (300 pg of *fz7/sfrp2/ror2/ror2 kd* and 100 pg of *wnt5a* per embryo) and the ATF2 firefly and pRL-TK *Renilla* luciferase reporter constructs. *B* and *C* show the mean ± S.D. of three independent experiments. *, p<0.05; **, p<0.001 compared with controls, Student's *t* test. *D* shows a representative with technical triplicates. This was confirmed by at least two independent experiments in different batches of *X. laevis* with similar results. *E* and *F* show the mean of 3 ± S.E. of biological triplicates of pools of five embryos each (*, *p* < 0.05 to controls). This was confirmed in at least two independent experiments in different batches of *X. laevis*.

xnr3 expression in AC explants by qPCR revealed that sFRP2 inhibits Wnt5a-NT7C5-induced *xnr3* expression (Fig. 5*B*). The inhibitory effect mediated by sFRP2 was also observed when Wnt11, an alternative ligand for Fz7, was used instead of Wnt5a (data not shown).

Previous data have shown that, apart from its interaction with Ror2 (45), the Fz7 receptor can also induce Ror2-independent Wnt/PCP signaling (11, 44). Thus, we analyzed whether Ror2 has an influence on classical Fz7-mediated signaling. We quantified *xnr3* expression in NT7C5-Ror2-injected AC

explants and observed that Ror2 completely blocked Wnt5a-NT7C5-mediated *xnr3* induction (Fig. 5*C*). To confirm that Ror2 inhibits Fz7 on the receptor level via direct interaction and not by its downstream signaling activity, we included a Ror2 kinase-dead (KD) mutant in this assay. This Ror2 mutant forms a complex with NT7C5 but has no signaling activity (18). As demonstrated in Fig. 5*C*, the KD mutant of Ror2 inhibited NT7C5-induced *xnr3* expression, indicating that the inhibition of Fz signaling is independent of Ror2 downstream signaling. As expected, *papc* expression was not induced by Ror2 KD (Fig. 5*D*). However, co-expression of WT Ror2 and NT7C5 strongly enhanced Ror2-mediated *papc* expression compared with the *papc* signal induced by Ror2 alone (Fig. 5*D*), supporting the idea that the extracellular portion of Fz7 is sufficient for enhancing Ror2 signaling. To further confirm that sFRP2 and Ror2 are negative regulators for Fz7, we used the ATF luciferase assay. Because the ATF reporter cannot discriminate between Fz7- and Ror2-induced signaling (Fig. 2*F*), we used the Ror2 KD construct in these experiments.

Consistently, we showed that sFRP2 inhibits Wnt5a-Fz7-mediated ATF reporter activity (Fig. 5*E*). Like sFRP2, Ror2 KD also inhibited Wnt5a-Fz7-induced reporter activity (Fig. 5*F*). Moreover, Ror2 KD was also able to inhibit Wnt11-Fz7-induced signaling (data not shown). Taken together, our results show that sFRP2 and Ror2 negatively influence Fz7-mediated signaling, whereas, at the same time, Ror2-mediated signaling is promoted by Fz7 and sFRP2.

sFRP2 and Ror2 Prevent Fz7 Receptor Endocytosis—Recent studies demonstrated that non-canonical Wnt signal transduction requires Fz receptor internalization (12). Consequently, we investigated whether sFRP2 or Ror2 have an effect on Fz7 localization and internalization. High-resolution *in vivo* imaging in zebrafish embryos has recently proven to be a valuable tool to study trafficking of Wnt ligands and receptors in a living vertebrate model organism (46, 47). By using this imaging-based *in vivo* approach, we observed that, in the absence of Wnt5a, Fz7 is localized at the cell membrane as well as in intracellular vesicles. After stimulation with Wnt5a, Fz7 is translocated from the membrane to intracellular vesicles (Fig. 6, *A* and *B*). However, co-injection of sFRP2 or Ror2 decreased Wnt5a-induced Fz7 receptor internalization. Instead, in the presence of Wnt5a, Fz7-CFP molecules form prominent clusters with Ror2-mCherry at the plasma membrane (Fig. 6*A*). These Ror2-Fz7 clusters were not observed when sFRP2, instead of Ror2, was co-expressed with Wnt5a and Fz7 (Fig. 6*A*). Moreover, this cluster formation is dependent on the presence of Wnt5a because Fz7 and Ror2 alone do not form clusters. In the absence of Wnt5a or Ror2, Fz7 is homogenously distributed at the membrane. To exclude that sFRP2 or Ror2 affect Wnt5a-V5 binding to Fz7, we performed IP experiments in HEK293T cells, demonstrating that both factors did not reduce or enhance Wnt5a binding to Fz7 (Fig. 6*C*).

To investigate whether the CRD motif alone is sufficient for Fz7 plasma membrane stabilization, we further analyzed the localization of Fz7 in the presence of the sFRP2-CRD. Confocal microscopy analysis showed that the CRD of sFRP2 alone was unable to prevent Wnt5a-induced stabilization of Fz7 at the membrane (Fig. 6, *D* and *E*). Notably, Fz7 vesicles seemed to be increased in size. These findings show that sFRP2 and Ror2 trap Fz7 at the cell membrane and reduce Fz7 receptor internalization. However, the CRD alone was unable to mimic the function of full-length sFRP2.

Taken together, our data support a novel role for sFRPs in the activation of distinct branches of the non-canonical signaling network. sFRPs activate Wnt5a-Ror2 signaling by stabilizing the ligand/receptor complex, and a stabilized Wnt5a-Ror2 complex inhibits Fz7-mediated signaling, most likely by inhibiting its endocytosis.

Discussion

Co-expression of Ror2 and Fz7 Leads to Mutually Exclusive Wnt Pathway Activation—A tight regulation of the different Wnt signaling cascades is crucial for proper cell migration during embryonic development. During *Xenopus* development, the receptors Fz7 and Ror2 are stimulated by the same ligand but can activate different downstream effectors and are suggested to mediate two distinct branches of β-catenin-independent Wnt signaling (4, 16, 48). However, it has also been shown that Fz7 and Ror2 co-operate to induce the activation of AP-1 *in vitro* (45). Using specific readouts for the distinct branches of Ror2 and Fz7, we were able to shed light on the molecular interplay of these two parallel pathways *in vivo*.

For Ror2-mediated signaling, we analyzed the expression of the target gene *papc* and found that Fz7 enhances Ror2-mediated signaling and is required for *papc* expression during *Xenopus* gastrulation (Fig. 4). This function is independent of the intracellular Fz domain because we also observed a stronger *papc* induction when the chimeric Fz7 receptor with a "canonical" signaling domain of Fz5 (NT7C5) was co-expressed with Ror2 (Fig. 5*D*). This suggests that the presence of an extracellular Fz-CRD motif promotes Ror2 activity. Surprisingly, we found that signal induction via the Fz7 receptor is repressed when both receptors are co-expressed. Using the chimeric NT7C5 receptor to monitor Fz7-mediated signaling, we observed that Ror2 inhibited Wnt5a-NT7C5-induced *xnr3* expression (Fig. 5*C*). This inhibition was not caused by downstream signaling components of Ror2, which inhibit Wnt/β-catenin signaling (49), because the kinase-inactive Ror2 mutant Ror2 KD (Fig. 5*D*) (16) also inhibited NT7C5 signaling (Fig. 5*C*). Thus, our data indicate that inhibition of Fz7 signaling by Ror2 occurs at the level of receptor complex formation. Taken together, our results demonstrate that interaction of Ror2 and Fz7 promotes Ror2-mediated signaling at the expense of Fz7 signaling.

sFRP2 Fine-tunes Signaling of Fz7 and Ror2 at the Receptor Level—Although there are several studies showing that sFRPs can act as Wnt signaling inhibitors (7, 8, 50–52), the mechanism of Wnt signal regulation by sFRPs is still unresolved. In our study, we demonstrate that sFRP2 is required for morphogenesis and co-localizes with the receptors Fz7 and Ror2 during *Xenopus* gastrulation (Fig. 4*E*). It differentially modulates the Ror2 pathway and Fz7-triggered signaling. We show that, similar to Ror2, sFRP2 inhibited Wnt5a-Fz7-mediated ATF activation and Wnt5a-NT7C5-induced *xnr3* expression (Fig. 5). Focusing on Ror2 signal transduction, we found that sFRP2, like Fz7, cooperates with Ror2 to induce Wnt5a-mediated *papc*
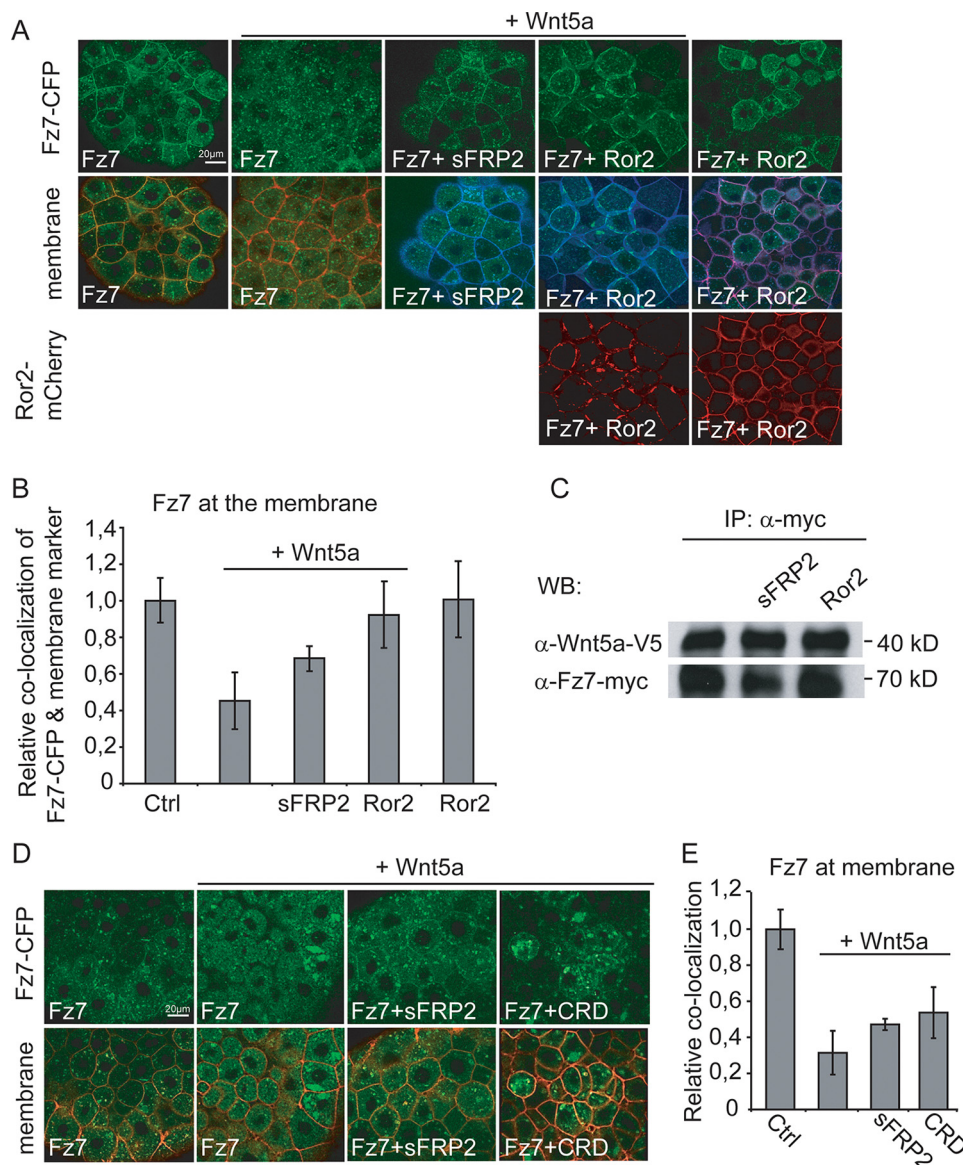
FIGURE 6. **sFRP2 and Ror2 inhibit Fz7 receptor endocytosis.** *A* and *D*, confocal microscopy analysis of live zebrafish embryos expressing 1 ng of mRNA of indicated constructs at 30–50% epiboly stage together with 1 ng of mRNA of the membrane marker mem-mCherry (*red*) or GFP-GPI (*blue*). Fz7-CFP (*green*) is present at the membrane and in endocytic vesicles. Co-expression of Wnt5a leads to enhanced internalization. sFRP2 as well as Ror2-mCherry are able to decrease Wnt5a-mediated endocytosis of Fz7-CFP. *B* and *E*, relative quantification of Fz7-CFP/membrane co-localization. *Ctrl* represents Fz7 alone. *C*, the Wnt5a-V5 binding assay was performed in HEK293T cells transfected with Fz7-myc alone or co-transfected with sFRP2-HA or Ror2-HA (1 μg of each). Each cell sample was treated with equal amounts of Wnt5a-V5 conditioned medium for 15 min before cells were lysed for rabbit anti-myc pulldown to precipitate Fz7. The samples were then analyzed on two different WBs. The WB on top was analyzed with anti-V5 antibody for the Wnt5a-V5 fraction bound to precipitated Fz7-myc. The bottom WB was analyzed with a mouse anti-myc and shows that equal amounts of Fz7-myc were precipitated in the different samples. *D*, co-expression of Wnt5a leads to enhanced internalization, which is repressed by full-length sFRP2 (also compare with *A*). The CRD of sFRP2 alone is unable to prevent Wnt5a-induced stabilization of Fz7 at the membrane but appears to increase the size of Fz7 vesicles.

expression (Fig. 2). We further show that sFRP2 and other sFRPs are required for *papc* expression during gastrulation (Fig. 4). This further supports our hypothesis that CRDs of Fz-related proteins promote and are required for Ror2 signal transduction.

Because of these findings, we focused on the function of the CRD in this process and provide insights into the potential mechanism of Ror2 signal regulation. Because the CRD of sFRP2 alone was able to enhance Wnt5a-V5 binding to Ror2 (Fig. 3C), we suggest that CRDs are responsible for Wnt5a-Ror2 stabilization and enhanced Ror2 signaling. Notably, Dkk3, which contains a cysteine-rich region distinct from those of

classical Fz and sFRP-CRDs (53), did not bind to Ror2 and had no effect on Wnt5a-Ror2 stabilization. The Fz7 receptor, however, is known to enhance Wnt5a binding to Ror2 (45), indicating that Ror2 signal transduction is specifically affected by Fz-CRDs.

Our finding that sFRPs stabilize Wnt5a-Ror2 complex formation is further consistent with the observation that sFRP2 increased Wnt5a puncta at the plasma membrane in zebrafish embryos (Fig. 3E). However, in the absence of sFRP2, there was constantly less Wnt5a-GFP detected in our experiments, which could indicate that Wnt5a-GFP is stabilized upon binding to a CRD of a receptor or an sFRP. This correlates with our data that
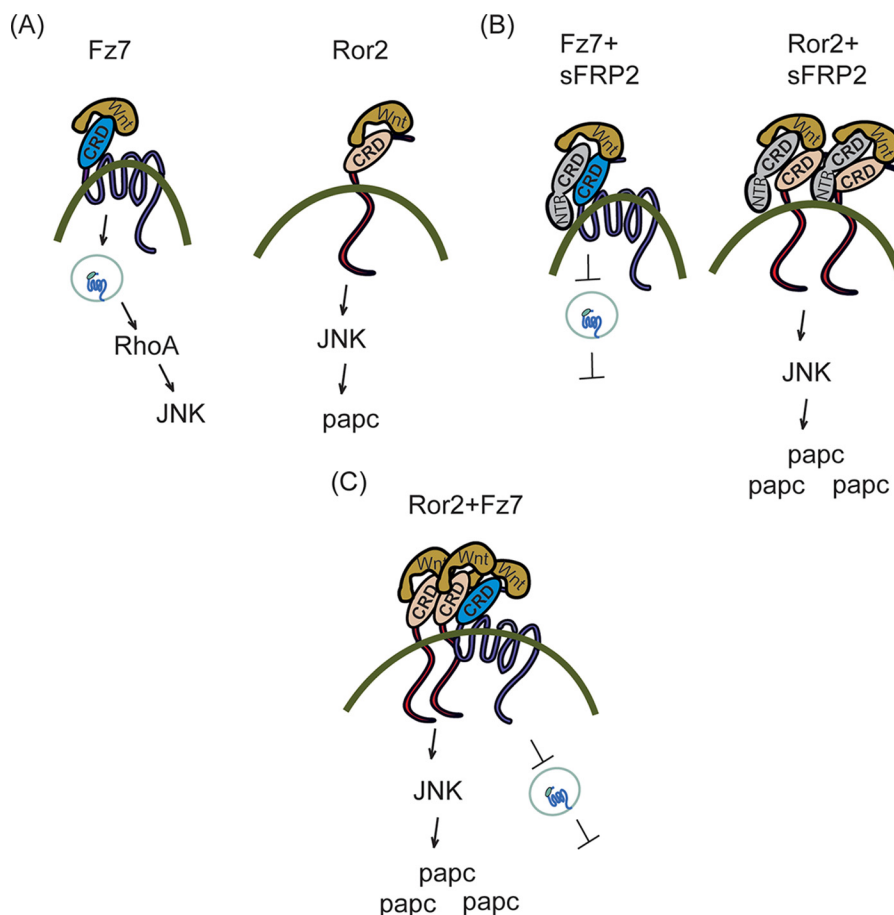
FIGURE 7. **Model for selective Fz7- or Ror2-mediated activation of non-canonical Wnt signaling.** *A,* when expressed alone, Fz7 or Ror2 receptors activate distinct non-canonical Wnt pathways stimulated by Wnt5a. *B,* when sFRP2 is present, Fz7 receptor endocytosis is prevented, and Fz7 signaling is inhibited, whereas Ror2 signaling is enhanced indicated by stabilized Wnt5a-Ror2 membrane complexes. *C,* when both receptors are present in the same cell, the Ror2-CRD acts in a similar way as sFRP2, leading to increased Ror2 activation at the expense of Fz7 signaling.

Ror2 signaling is much lower when only Wnt5a was co-expressed (Fig. 2*E*). Of note, we could not observe an additional increase of Ror2 activity using higher concentrations of sFRP2 (data not shown), indicating that sFRP2 might modulate Wnt signaling in a biphasic manner and might form inactive clusters at high concentrations. Consistently, data published previously by us showed that increasing amounts of soluble mouse Fz8-CRD modulated Wnt3a-induced signaling in a biphasic manner, and micromolar CRD concentrations were proposed to form inactive Wnt-CRD polymers (2).

Taken together, we show that sFRP2 is necessary to regulate morphogenic movements during *Xenopus* gastrulation. sFRP2 inhibits Fz7 but augments Ror2 signaling, suggesting that sFRP2 balances the signaling activities of Ror2 and Fz7. We further demonstrate that the CRD of sFRP2 is sufficient to stabilize Wnt5a-Ror2 complexes at the membrane and thereby promotes Ror2 signal transduction.

sFRP2 and Ror2 Block Fz7 Receptor Internalization—To get more insights into the mechanism of Fz7 receptor inhibition, we further investigated whether Ror2 or sFRP2 might have an influence on the subcellular localization of Fz7. Several reports focusing on endocytosis demonstrated that the internalization of Fz receptors plays a crucial role in transducing the non-canonical Wnt signal (13, 34). Our data confirm that, in zebrafish,

Wnt5a induces the formation of intracellular Fz7 vesicles (Fig. 6, *A* and *B*). This vesicle formation is strongly reduced when Ror2 is co-expressed, demonstrating that Ror2 is able to retain Fz7 at the cell membrane. Moreover, Ror2 and Fz7 form prominent clusters when Wnt5a was co-expressed, assuming that Ror2-Fz7 cluster formation and complex stabilization depends on the presence of Wnt. When relying on overexpression analysis, the observed Wnt5a-induced Ror2-Fz7 cluster formation is in line with previous findings that Wnt5a stimulates Ror2 clustering at the cell membrane in *Xenopus* tissues (37) and, further, that Wnt5a enhances Fz7 binding to Ror2 (45). However, it was shown that the CRD of Ror2 enhances Fz7-mediated clustering of Dvl2, which co-localizes with the Wnt-PCP effector Rac1, suggesting that Ror2 supports Fz7-triggered signaling (45). At first glance this is contrary to the inhibition of Fz7-specific signaling by Ror2 observed in our study. Still, it is not yet known whether the formation of Dvl2-Rac1 clusters alone is sufficient to activate signaling in mouse L cells or whether these need to be internalized in complex with Fz7 to induce Wnt signaling. It remains to be shown whether Fz7 is also part of the observed Dvl2-Rac1 complex or whether Ror2, as in our study, traps Fz7 at the membrane and induces AP-1 via an alternative and Rac1-independent pathway, as shown for *Xenopus* (16). Furthermore, the interaction of Fz7 and Ror2

could have different, context-dependent effects in distinct cell lines and tissues. As an example, Ryk (atypical receptor-related tyrosine kinase) was demonstrated to function as a co-receptor for Fz7 to promote Wnt11-mediated endocytosis of Dsh (13). Ryk is a single-pass transmembrane protein with a WIF motif unrelated to Fz-CRDs and maternally provided in *Xenopus*. Ror2, which is strongly up-regulated during gastrulation, might compete with Ryk in mesodermal tissue for Fz7 binding to antagonize their cooperating effects. Similar to this, the type of co-receptors expressed in a given tissue could determine whether Fz internalization and signaling is repressed or promoted.

In addition to Ror2, sFRP2 was also able to stabilize Fz7 at the cell membrane in zebrafish (Fig. 6, *A* and *B*). However, sFRP2 did not induce the strong Fz7 cluster formation seen in Ror2-treated animals, suggesting that the transmembrane and intracellular domains of Ror2 might serve as an anchor for Fz7. The effect induced by sFRP2 is much weaker. At present, it is unclear how sFRP2 prevents Fz7 receptor endocytosis. The NTR domain of sFRP was suggested to interact with heparin and therefore might be responsible for sFRP association with the cell membrane (54, 55). Indeed, we found that sFRP2, lacking the NTR domain was less potent in stabilizing Fz7 at the membrane (Fig. 6, *D* and *E*), indicating that the NTR domain of sFRP2 might be instrumental for efficient Fz7 receptor stabilization. Preliminary data obtained by live-cell imaging indicate that non-canonical Wnt-Ror2 complexes are internalized in a caveolin-dependent manner, whereas Fz7 signaling, conversely, was affected by clathrin-specific inhibitors (data not shown). These mechanisms, however, have to be addressed in more detail in future studies. Collectively, we show that sFRP2 and Ror2 prevent Fz7 receptor endocytosis, which could provide a mechanism for the observed inhibition of Fz7 signal transduction.

In conclusion, our study demonstrates that the CRD motif in sFRPs can act as a molecular switch to promote or repress specific β-catenin-independent Wnt signaling branches. On the basis of our data we propose following model. When each receptor is expressed alone and stimulated with Wnt5a, Ror2 signaling is mildly stimulated, and the Fz7 receptor is internalized, thereby activating the Fz7 signaling pathway (Fig. 7*A*). However, when sFRP2 is present in the extracellular space, it binds to Ror2 via its CRD and stabilizes Wnt5a-Ror2 complexes, leading to a high Ror2 signaling activity (Fig. 7*B*). On the other hand, when sFRP2 binds to Fz7, this complex is stabilized at the cell membrane, preventing Fz7 endocytosis and thereby reducing Fz7 signaling (Fig. 7*B*). Independent of sFRP2, when both receptors are co-expressed, they can directly interact and influence the signaling activity of the other, leading to enhanced Ror2 and reduced Fz7 signaling. The CRD of the corresponding receptor thereby substitutes the CRD of sFRP2 (Fig. 7*C*).

How can the divergent effects of sFRPs in different receptor contexts be explained? CRD-CRD interactions appear to be at the core of this regulatory mechanism. Our data suggest that CRD heterodimers formed by the Ror2-CRD enhance signaling via this route, whereas Fz7 heterodimers formed with Ror2 or sFRP-CRDs inhibit signaling and endocytosis of Fz7. On the other hand, forced Fz7 homodimerization has been shown to

induce canonical Wnt signaling. PCP signaling via Fz7 might therefore be generally inhibited by Wnt ligand binding to a Fz7 with a dimeric CRD configuration, which probably precludes association with membrane-bound or cytoplasmic factors specific for the Fz-Rho signaling pathway (11). To solve this hypothesis, the role of the receptor-ligand stoichiometry in different non-canonical Wnt signaling cascades and the effect of sFRPs on complex composition should be the focus of future studies.

References

1. Janda, C. Y., Waghray, D., Levin, A. M., Thomas, C., and Garcia, K. C. (2012) Structural basis of Wnt recognition by Frizzled. *Science* **337,** 59–64
2. Kumar, S., Žigman, M., Patel, T. R., Trageser, B., Gross, J. C., Rahm, K., Boutros, M., Gradl, D., Steinbeisser, H., Holstein, T., Stetefeld, J., and Özbek, S. (2014) Molecular dissection of Wnt3a-Frizzled8 interaction reveals essential and modulatory determinants of Wnt signaling activity. *BMC Biol.* **12,** 44
3. Dann, C. E., Hsieh, J. C., Rattner, A., Sharma, D., Nathans, J., and Leahy, D. J. (2001) Insights into Wnt binding and signalling from the structures of two Frizzled cysteine-rich domains. *Nature* **412,** 86–90
4. Niehrs, C. (2012) The complex world of WNT receptor signalling. *Nat. Rev. Mol. Cell Biol.* **13,** 767–779
5. Malinauskas, T., and Jones, E. Y. (2014) Extracellular modulators of Wnt signalling. *Curr. Opin. Struct. Biol.* **29,** 77–84
6. Kawano, Y., and Kypta, R. (2003) Secreted antagonists of the Wnt signalling pathway. *J. Cell Sci.* **116,** 2627–2634
7. Leyns, L., Bouwmeester, T., Kim, S. H., Piccolo, S., and De Robertis, E. M. (1997) Frzb-1 is a secreted antagonist of Wnt signaling expressed in the Spemann organizer. *Cell* **88,** 747–756
8. Lin, K., Wang, S., Julius, M. A., Kitajewski, J., Moos, M., Jr., and Luyten, F. P. (1997) The cysteine-rich frizzled domain of Frzb-1 is required and sufficient for modulation of Wnt signaling. *Proc. Natl. Acad. Sci. U.S.A.* **94,** 11196–11200
9. Wawrzak, D., Métioui, M., Willems, E., Hendrickx, M., de Genst, E., and Leyns, L. (2007) Wnt3a binds to several sFRPs in the nanomolar range. *Biochem. Biophys. Res. Commun.* **357,** 1119–1123
10. Wang, Y., and Steinbeisser, H. (2009) Molecular basis of morphogenesis during vertebrate gastrulation. *Cell Mol. Life Sci.* **66,** 2263–2273
11. Habas, R., Dawid, I. B., and He, X. (2003) Coactivation of Rac and Rho by Wnt/Frizzled signaling is required for vertebrate gastrulation. *Genes Dev.* **17,** 295–309
12. Yu, A., Xing, Y., Harrison, S. C., and Kirchhausen, T. (2010) Structural analysis of the interaction between Dishevelled2 and clathrin AP-2 adaptor, a critical step in noncanonical Wnt signaling. *Structure* **18,** 1311–1320
13. Kim, G. H., Her, J. H., and Han, J. K. (2008) Ryk cooperates with Frizzled 7 to promote Wnt11-mediated endocytosis and is essential for *Xenopus laevis* convergent extension movements. *J. Cell Biol.* **182,** 1073–1082
14. Oishi, I., Suzuki, H., Onishi, N., Takada, R., Kani, S., Ohkawara, B., Ko-

shida, I., Suzuki, K., Yamada, G., Schwabe, G. C., Mundlos, S., Shibuya, H., Takada, S., and Minami, Y. (2003) The receptor tyrosine kinase Ror2 is involved in non-canonical Wnt5a/JNK signalling pathway. *Genes Cells* **8,** 645–654

15. Minami, Y., Oishi, I., Endo, M., and Nishita, M. (2010) Ror-family receptor tyrosine kinases in noncanonical Wnt signaling: their implications in developmental morphogenesis and human diseases. *Dev. Dyn.* **239,** 1–15

16. Schambony, A., and Wedlich, D. (2007) Wnt-5A/Ror2 regulate expression of XPAPC through an alternative noncanonical signaling pathway. *Dev. Cell* **12,** 779–792

17. Djiane, A., Riou, J., Umbhauer, M., Boucaut, J., and Shi, D. (2000) Role of frizzled 7 in the regulation of convergent extension movements during gastrulation in *Xenopus laevis*. *Development* **127,** 3091–3100

18. Hikasa, H., Shibata, M., Hiratani, I., and Taira, M. (2002) The *Xenopus* receptor tyrosine kinase Xror2 modulates morphogenetic movements of the axial mesoderm and neuroectoderm via Wnt signaling. *Development* **129,** 5227–5239

19. Kim, S. H., Jen, W. C., De Robertis, E. M., and Kintner, C. (2000) The protocadherin PAPC establishes segmental boundaries during somitogenesis in *Xenopus* embryos. *Curr. Biol.* **10,** 821–830

20. Kim, S. H., Yamamoto, A., Bouwmeester, T., Agius, E., and Robertis, E. M. (1998) The role of paraxial protocadherin in selective adhesion and cell movements of the mesoderm during *Xenopus* gastrulation. *Development* **125,** 4681–4690

21. Satoh, W., Gotoh, T., Tsunematsu, Y., Aizawa, S., and Shimono, A. (2006) Sfrp1 and Sfrp2 regulate anteroposterior axis elongation and somite segmentation during mouse embryogenesis. *Development* **133,** 989–999

22. Satoh, W., Matsuyama, M., Takemura, H., Aizawa, S., and Shimono, A. (2008) Sfrp1, Sfrp2, and Sfrp5 regulate the Wnt/β-catenin and the planar cell polarity pathways during early trunk formation in mouse. *Genesis* **46,** 92–103

23. Li, Y., Rankin, S. A., Sinner, D., Kenny, A. P., Krieg, P. A., and Zorn, A. M. (2008) Sfrp5 coordinates foregut specification and morphogenesis by antagonizing both canonical and noncanonical Wnt11 signaling. *Genes Dev.* **22,** 3050–3063

24. Sugiyama, Y., Stump, R. J., Nguyen, A., Wen, L., Chen, Y., Wang, Y., Murdoch, J. N., Lovicu, F. J., and McAvoy, J. W. (2010) Secreted frizzled-related protein disrupts PCP in eye lens fiber cells that have polarised primary cilia. *Dev. Biol.* **338,** 193–201

25. Swain, R. K., Medina, A., and Steinbeisser, H. (2001) Functional analysis of the *Xenopus* frizzled 7 protein domains using chimeric receptors. *Int. J. Dev. Biol.* **45,** 259–264

26. Medina, A., and Steinbeisser, H. (2000) Interaction of Frizzled 7 and Dishevelled in *Xenopus*. *Dev. Dyn.* **218,** 671–680

27. Moon, R. T., Campbell, R. M., Christian, J. L., McGrew, L. L., Shih, J., and Fraser, S. (1993) Xwnt-5A: a maternal Wnt that affects morphogenetic movements after overexpression in embryos of *Xenopus laevis*. *Development* **119,** 97–111

28. Du, S. J., Purcell, S. M., Christian, J. L., McGrew, L. L., and Moon, R. T. (1995) Identification of distinct classes and functional domains of Wnts through expression of wild-type and chimeric proteins in *Xenopus* embryos. *Mol. Cell. Biol.* **15,** 2625–2634

29. Winklbauer, R., Medina, A., Swain, R. K., and Steinbeisser, H. (2001) Frizzled-7 signalling controls tissue separation during *Xenopus* gastrulation. *Nature* **413,** 856–860

30. Gibb, N., Lavery, D. L., and Hoppler, S. (2013) sfrp1 promotes cardiomyocyte differentiation in *Xenopus* via negative-feedback regulation of Wnt signalling. *Development* **140,** 1537–1549

31. Shibata, M., Itoh, M., Hikasa, H., Taira, S., and Taira, M. (2005) Role of crescent in convergent extension movements by modulating Wnt signaling in early *Xenopus* embryogenesis. *Mech. Dev.* **122,** 1322–1339

32. Medina, A., Swain, R. K., Kuerner, K. M., and Steinbeisser, H. (2004) *Xenopus* paraxial protocadherin has signaling functions and is involved in tissue separation. *EMBO J.* **23,** 3249–3258

33. Perry, S. W., Epstein, L. G., and Gelbard, H. A. (1997) *In situ* trypan blue staining of monolayer cell cultures for permanent fixation and mounting. *BioTechniques* **22,** 1020–1021, 1024

34. Ohkawara, B., Glinka, A., and Niehrs, C. (2011) Rspo3 binds syndecan 4 and induces Wnt/PCP signaling via clathrin-mediated endocytosis to promote morphogenesis. *Dev. Cell* **20,** 303–314

35. Brand, M., Granato, M., and Nüsslein-Volhard, C. (2002) Keeping and raising zebrafish. In *Zebrafish: A Practical Approach* (Nüsslein-Volhard, C., and Dahm, R., eds) pp. 7–38, Oxford University Press, Oxford, UK

36. Witzel, S., Zimyanin, V., Carreira-Barbosa, F., Tada, M., and Heisenberg, C. P. (2006) Wnt11 controls cell contact persistence by local accumulation of Frizzled 7 at the plasma membrane. *J. Cell Biol.* **175,** 791–802

37. Wallkamm, V., Dörlich, R., Rahm, K., Klessing, T., Nienhaus, G. U., Wedlich, D., and Gradl, D. (2014) Live imaging of Xwnt5A-ROR2 complexes. *PLoS ONE* **9,** e109428

38. Rengarajan, C., Matzke, A., Reiner, L., Orian-Rousseau, V., and Scholpp, S. (2014) Endocytosis of Fgf8 is a double-stage process and regulates spreading and signaling. *PLoS ONE* **9,** e86373

39. Pera, E. M., and De Robertis, E. M. (2000) A direct screen for secreted proteins in *Xenopus* embryos identifies distinct activities for the Wnt antagonists Crescent and Frzb-1. *Mech. Dev.* **96,** 183–195

40. Medina, A., Reintsch, W., and Steinbeisser, H. (2000) *Xenopus* frizzled 7 can act in canonical and non-canonical Wnt signaling pathways: implications on early patterning and morphogenesis. *Mech. Dev.* **92,** 227–237

41. Itoh, K., Jacob, J., and Y Sokol, S. (1998) A role for *Xenopus* Frizzled 8 in dorsal development. *Mech. Dev.* **74,** 145–157

42. Sumanas, S., and Ekker, S. C. (2001) *Xenopus* frizzled-7 morphant displays defects in dorsoventral patterning and convergent extension movements during gastrulation. *Genesis* **30,** 119–122

43. Isaacs, H. V., Pownall, M. E., and Slack, J. M. (1994) eFGF regulates Xbra expression during *Xenopus* gastrulation. *EMBO J.* **13,** 4469–4481

44. Ohkawara, B., and Niehrs, C. (2011) An ATF2-based luciferase reporter to monitor non-canonical Wnt signaling in *Xenopus* embryos. *Dev. Dyn.* **240,** 188–194

45. Nishita, M., Itsukushima, S., Nomachi, A., Endo, M., Wang, Z., Inaba, D., Qiao, S., Takada, S., Kikuchi, A., and Minami, Y. (2010) Ror2/Frizzled complex mediates Wnt5a-induced AP-1 activation by regulating Dishevelled polymerization. *Mol. Cell. Biol.* **30,** 3610–3619

46. Hagemann, A. I., Kurz, J., Kauffeld, S., Chen, Q., Reeves, P. M., Weber, S., Schindler, S., Davidson, G., Kirchhausen, T., and Scholpp, S. (2014) *In vivo* analysis of formation and endocytosis of the Wnt/β-catenin signaling complex in zebrafish embryos. *J. Cell Sci.* **127,** 3970–3982

47. Stanganello, E., Hagemann, A. I., Mattes, B., Sinner, C., Meyen, D., Weber, S., Schug, A., Raz, E., and Scholpp, S. (2015) Filopodia-based Wnt transport during vertebrate tissue patterning. *Nat. Commun.* **6,** 5846

48. Ho, H. Y., Susman, M. W., Bikoff, J. B., Ryu, Y. K., Jonas, A. M., Hu, L., Kuruvilla, R., and Greenberg, M. E. (2012) Wnt5a-Ror-Dishevelled signaling constitutes a core developmental pathway that controls tissue morphogenesis. *Proc. Natl. Acad. Sci. U.S.A.* **109,** 4044–4051

49. Yuan, Y., Niu, C. C., Deng, G., Li, Z. Q., Pan, J., Zhao, C., Yang, Z. L., and Si, W. K. (2011) The Wnt5a/Ror2 noncanonical signaling pathway inhibits canonical Wnt signaling in K562 cells. *Int. J. Mol. Med.* **27,** 63–69

50. Uren, A., Reichsman, F., Anest, V., Taylor, W. G., Muraiso, K., Bottaro, D. P., Cumberledge, S., and Rubin, J. S. (2000) Secreted frizzled-related protein-1 binds directly to Wingless and is a biphasic modulator of Wnt signaling. *J. Biol. Chem.* **275,** 4374–4382

51. Bhat, R. A., Stauffer, B., Komm, B. S., and Bodine, P. V. (2007) Structure-function analysis of secreted frizzled-related protein-1 for its Wnt antagonist function. *J. Cell. Biochem.* **102,** 1519–1528

52. Lopez-Rios, J., Esteve, P., Ruiz, J. M., and Bovolenta, P. (2008) The Netrin-related domain of Sfrp1 interacts with Wnt ligands and antagonizes their activity in the anterior neural plate. *Neural Dev.* **3,** 19

53. Cruciat, C. M., and Niehrs, C. (2013) Secreted and transmembrane wnt inhibitors and activators. *Cold Spring Harb. Perspect. Biol.* **5,** a015081

54. Finch, P. W., He, X., Kelley, M. J., Uren, A., Schaudies, R. P., Popescu, N. C., Rudikoff, S., Aaronson, S. A., Varmus, H. E., and Rubin, J. S. (1997) Purification and molecular cloning of a secreted, Frizzled-related antagonist of Wnt action. *Proc. Natl. Acad. Sci. U.S.A.* **94,** 6770–6775

55. Chong, J. M., Uren, A., Rubin, J. S., and Speicher, D. W. (2002) Disulfide bond assignments of secreted Frizzled-related protein-1 provide insights about Frizzled homology and netrin modules. *J. Biol. Chem.* **277,** 5134–5144

Access the most updated version of this article at doi: 10.1074/jbc.M116.733766

Alerts:
- When this article is cited
- When a correction for this article is posted

Click here to choose from all of JBC's e-mail alerts

This article cites 54 references, 21 of which can be accessed free at
http://www.jbc.org/content/291/26/13730.full.html#ref-list-1